Supporting information:

Thermal structural stability of multi-component olivine electrode for lithium ion batteries

Kyu-Young Park [†,a, b], Hyungsub Kim [†,a, c], Seongsu Lee[c], Jongsoon Kim[c], Jihyun Hong [a], Hee-Dae Lim [a, b], Inchul Park [a, b] and Kisuk Kang [a, b, *]

[a] Department of Materials Science and Engineering, Research Institute of Advanced Materials (RIAM), Seoul National University, 599 Gwanak-ro, Gwanak-gu, Seoul 151-742, Republic of Korea

[b] Center for Nanoparticle Research, Institute for Basic Science (IBS), Seoul National University, Seoul 151-742, Republic of Korea

[c] Korea Atomic Energy Research Institute, P.O. Box 105, Daejeon 305-600, Republic of Korea

[†] These authors contributed equally.

*Corresponding Author. Tel.: +82-2-880-7088 Fax.: +82-2-885-9671 E-mail address: matlgen1@snu.ac.kr

Table S1. Elemental composition ratios in multi-component olivine using inductively coupled plasma mass spectroscopy (ICP-MS) analyses.

Sample	Li	Mn	Fe	Co
Li = 1	98.6	32.8	33.6	33.6
Li = 2/3	63.4	35.3	36.4	28.3
Li = 1/2	53.2	33.2	37.3	29.5
Li = 1/3	34.8	34.8	35.6	29.6
Li = 0	5.1	35.2	37.8	27

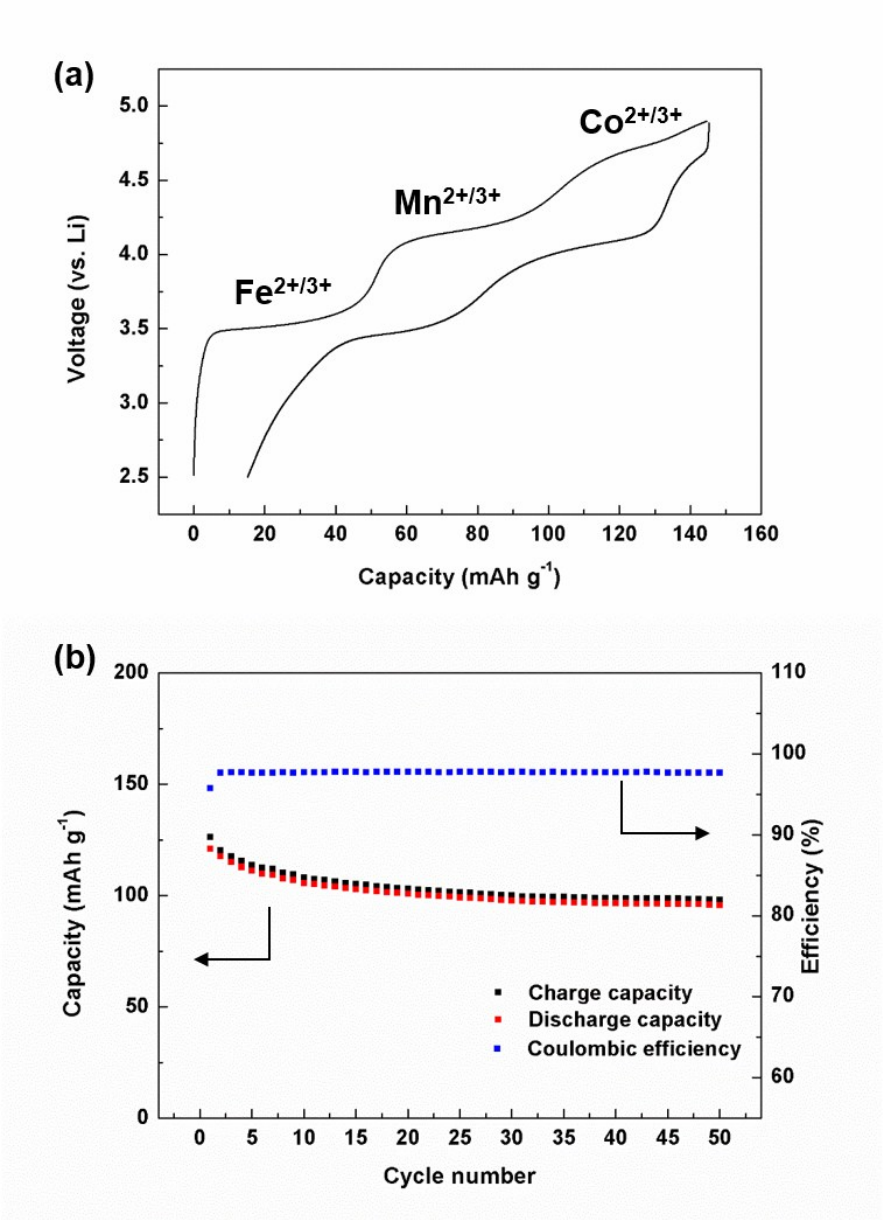

Fig. S1. (a) Galvanostatic charge/discharge profile of $LiMn_{1/3}Fe_{1/3}Co_{1/3}PO_4$ at a current density of 10 mA g^{-1}. (b) Cycle life test of $LiMn_{1/3}Fe_{1/3}Co_{1/3}PO_4$ with a current density 0.2 A g^{-1} (Corresponding to 1.18 C). The capacity after 50 cycles maintained 76 % of the initial charge/discharge capacity. The electrochemical cells were assembled using a CR2032-typte coin-cell with Li metal as the counter electrode. An electrolyte of 1 M $LiPF_6$ in ethyl carbonate/dimethyl carbonate (Panax, EC/DMC, 1:1 v/v) were used in the cell fabrication.

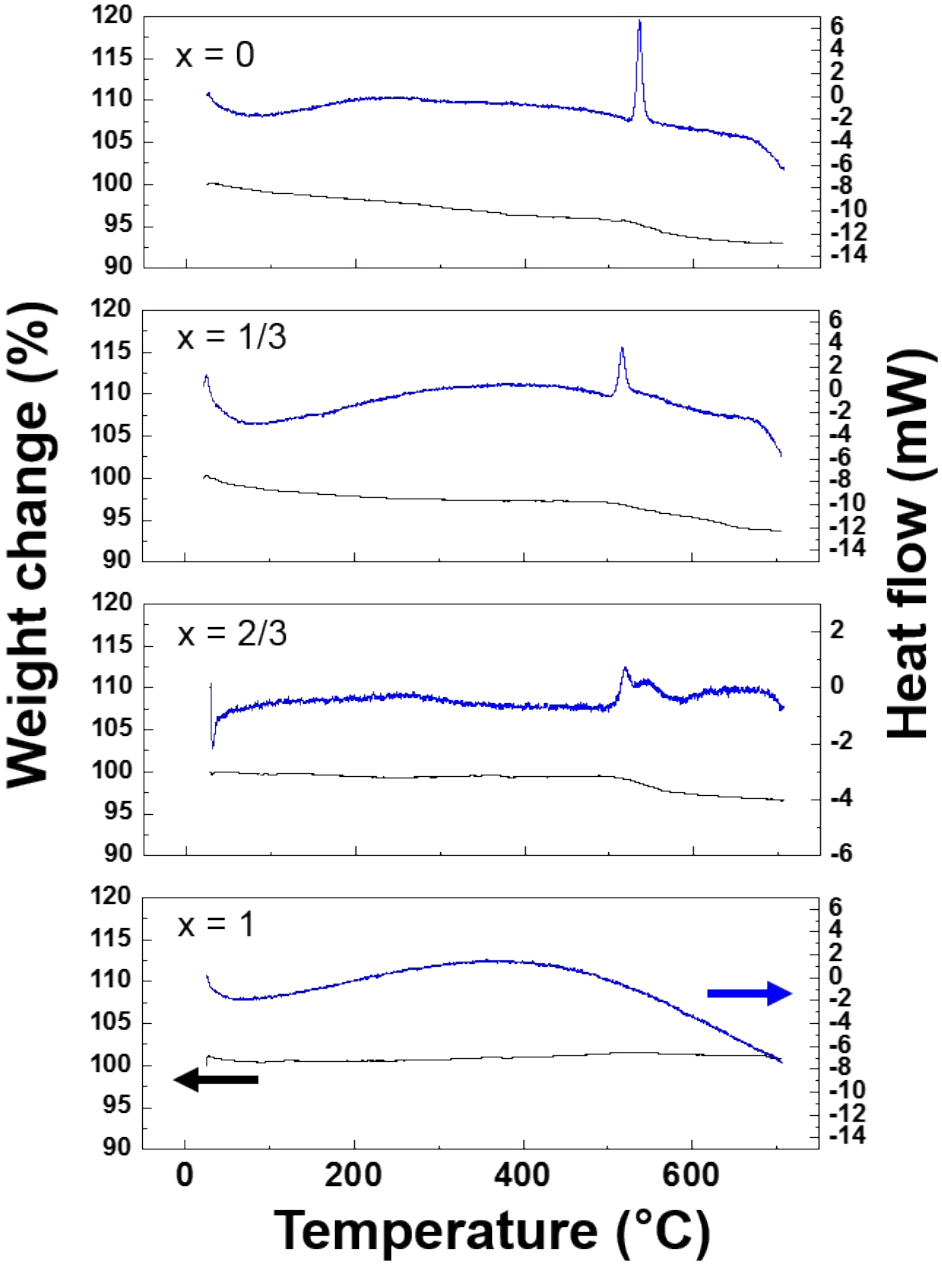

Fig. S2. Thermogravimetric Analysis / Differential Scanning. Calorimetry (TGA/DSC) profiles of $Li_xMn_{1/3}Fe_{1/3}Co_{1/3}PO_4$ (x = 0, 1/3, 2/3 and 1). The black and blue line illustrate the TGA and DSC profiles, respectively.

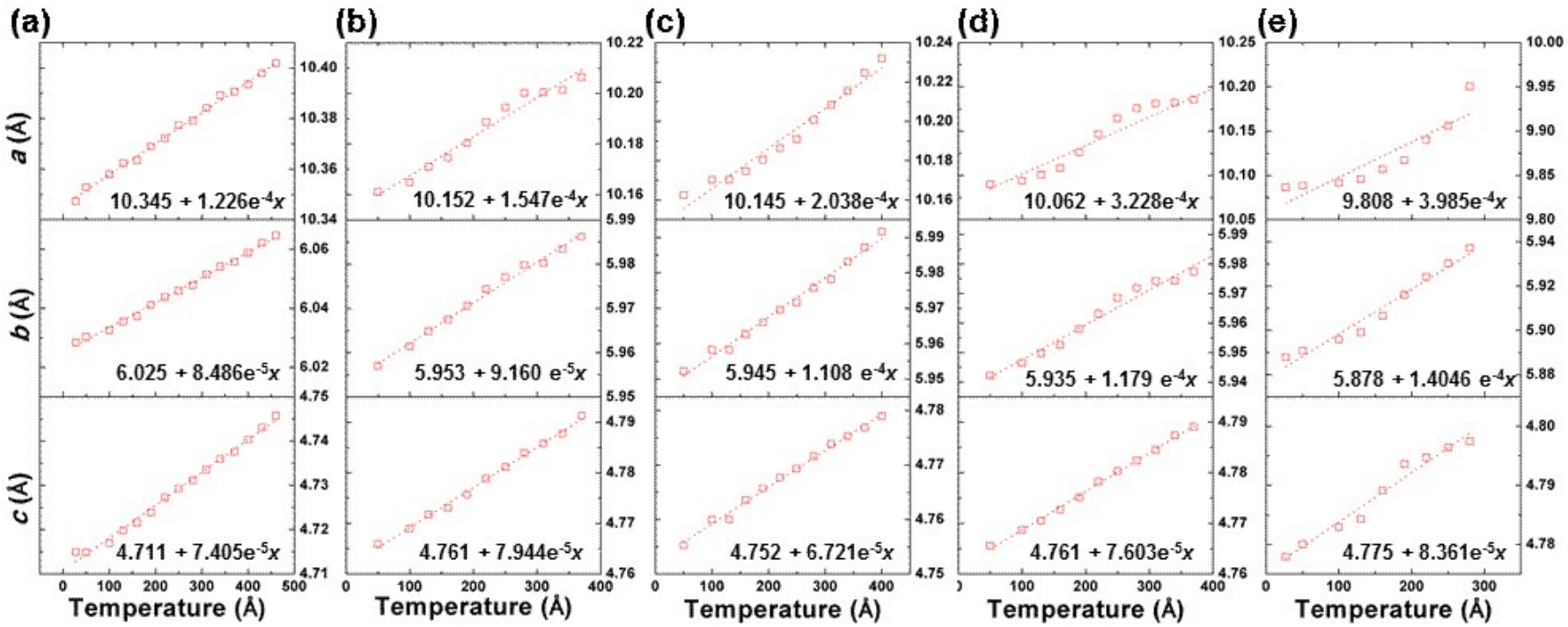

Fig. S3. Lattice parameter change of $Li_xMn_{1/3}Fe_{1/3}Co_{1/3}PO4$ ((a) $x = 1$, (b) $x = 2/3$, (c) $x = 1/2$, (d) $x = 1/3$, (e) $x = 0$) as a function of temperature. The thermal coefficients are estimated from linear square fitting.

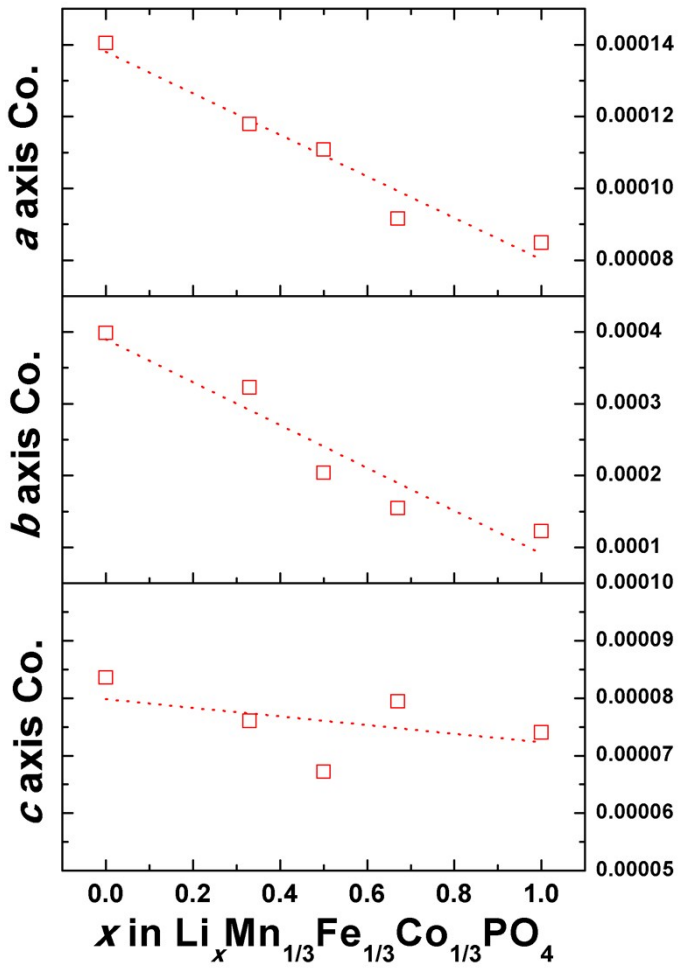

Fig. S4. Thermal coefficient variation of $Li_xFe_{1/3}Mn_{1/3}Co_{1/3}PO_4$ ($0 \le x \le 1$) as a function of Li contents.

Table S2. (a) Detailed structural information of $LiMn_{1/3}Fe_{1/3}Co_{1/3}PO_4$ from Rietveld refinement of the neutron diffraction pattern at room temperature.

Formula	$LiMn_{1/3}Fe_{1/3}Co_{1/3}PO_4$
Crystal system	Orthorhombic
Space group	Pnma (No. 62)
Lattice parameters	
a (Å)	10.3222 (3)
b (Å)	6.0088 (2)
c (Å)	4.7126 (1)
Unitcell volume ($Å^3$)	297.29 (1)
Source	Neutron
Temperature (K)	300K
Wave length (Å)	1.834333
2θ range	0 – 180°
Number of data points	3200
Number of reflections	203
R_p (%)	2.07 %
R_{wp} (%)	2.71 %
R_I (%)	3.52 %
R_F (%)	2.52 %

$LiMn_{1/3}Fe_{1/3}Co_{1/3}PO_4$

Atom	*x* (Å)	*y* (Å)	*z* (Å)	B_{iso}	Occupancy
Li1	0	0	0	-	1.0
Fe	0.2780(4)	0.25	0.9667(10)	1.45(8)	0.336
Mn	0.2780(4)	0.25	0.9667(10)	1.45(8)	0.328
Co	0.2780(4)	0.25	0.9667(10)	1.45(8)	0.336
P	0.09326(19)	0.25	0.4123(4)	-	1.0
O1	0.09838(19)	0.25	0.7380(4)	-	1.0
O2	0.45590(17)	0.25	0.2031(4)	-	1.0
O3	0.16371(15)	0.0470(2)	0.2809(3)	-	1.0

Atom	U_{11} (Å^2)	U_{22} (Å^2)	U_{33} (Å^2)	U_{12} (Å^2)	U_{13} (Å^2)	U_{23} (Å^2)
Li1	0.025(4)	0.033(4)	0.020(4)	0.002(3)	0.005(4)	-0.009(3)
P	0.0026(11)	0.0158(11)	0.0036(9)	0	0.0068(10)	0
O1	0.0134(9)	0.0092(9)	0.0044(14)	0	0.0041(10)	0
O2	0.0185(11)	0.0087(9)	0.0048(12)	0	-0.0007(9)	0
O3	0.0152(8)	0.0055(6)	0.0116(9)	0.0043(6)	-0.0006(7)	-0.0049(7)

Formula	$Li_{2/3}Mn_{1/3}Fe_{1/3}Co_{1/3}PO_4$	$Li_{1/2}Mn_{1/3}Fe_{1/3}Co_{1/3}PO_4$	$Li_{1/3}Mn_{1/3}Fe_{1/3}Co_{1/3}PO_4$
Crystal system	Orthorhombic	Orthorhombic	Orthorhombic
Space group	Pnma (No. 62)	Pnma (No. 62)	Pnma (No. 62)
Lattice parameters			
a (Å)	10.1738 (5)	10.1554 (4)	10.0846 (6)
b (Å)	5.9568 (3)	5.9501 (2)	5.9397 (4)
c (Å)	4.7604 (2)	4.7636 (2)	4.7690 (3)
Volume ($Å^3$)	288.50 (2)	287.85 (2)	285.66 (3)
Source	Neutron	Neutron	Neutron
Temperature (K)	300K	300K	300K
Wave length (Å)	1.834333	1.834333	1.834333
2θ range	0 – 180°	0 – 180°	0 – 180°
Number of data points	3200	3200	3200
Number of reflections	216	216	216
R_p (%)	1.96 %	1.52 %	1.61 %
R_{wp} (%)	2.51 %	1.93 %	2.05 %
R_I (%)	1.89 %	1.97 %	2.35 %
R_F (%)	1.22 %	1.39 %	1.61 %

$Li_{2/3}Mn_{1/3}Fe_{1/3}Co_{1/3}PO_4$

Atom	*x* (Å)	*y* (Å)	*z* (Å)	B_{iso}	Occupancy
Li1	0	0	0	0.7(2)	0.63
Fe	0.2758(5)	0.25	0.9839(12)	1.64(12)	0.364
Mn	0.2758(5)	0.25	0.9839(12)	1.64(12)	0.353
Co	0.2758(5)	0.25	0.9839(12)	1.64(12)	0.283
P	0.0950(3)	0.25	0.4137(5)	-	1.0
O1	0.1077(2)	0.25	0.7316(5)	-	1.0
O2	0.4533(2)	0.25	0.1849(5)	-	1.0
O3	0.1674(2)	0.0473(3)	0.2767(4)	-	1.0

Atom	U_{11} (Å^2)	U_{22} (Å^2)	U_{33} (Å^2)	U_{12} (Å^2)	U_{13} (Å^2)	U_{23} (Å^2)
P	0.0038(3)	0.0048(8)	0.0130(1)	0	-0.0024(7)	0
O1	0.0022(3)	0.0104(7)	0.0053(1)	0	-0.0014(5)	0
O2	0.0019(3)	0.0125(9)	0.015 (1)	0	0.0011(4)	0
O3	0.0032(2)	0.0080(4)	0.0110(1)	0.00095	0.0023(4)	-0.0022(8)

$Li_{1/2}Mn_{1/3}Fe_{1/3}Co_{1/3}PO_4$

Atom	*x* (Å)	*y* (Å)	*z* (Å)	B_{iso}	Occupancy
Li1	0	0	0	0.3(2)	0.552
Fe	0.2752(4)	0.25	0.9792(11)	2.13(11)	0.373
Mn	0.2752(4)	0.25	0.9792(11)	2.13(11)	0.332
Co	0.2752(4)	0.25	0.9792(11)	2.13(11)	0.295
P	0.0948(3)	0.25	0.4133(5)	-	1.0
O1	0.1076(2)	0.25	0.7317(4)	-	1.0
O2	0.4527(2)	0.25	0.1838(4)	-	1.0
O3	0.16723(19)	0.0480(2)	0.2763(4)	-	1.0

Atom	U_{11} (Å^2)	U_{22} (Å^2)	U_{33} (Å^2)	U_{12} (Å^2)	U_{13} (Å^2)	U_{23} (Å^2)
P	0.0040(3)	0.0046(7)	0.0108(8)	0	-0.0031(6)	0
O1	0.0023(3)	0.0096(6)	0.011(1)	0	-0.0009(5)	0
O2	0.0017(2)	0.0118(8)	0.020(1)	0	0.0018(4)	0
O3	0.0042(2)	0.0087(4)	0.0098(9)	0.0020(3)	0.0019(3)	0.0002(7)

$Li_{1/3}Mn_{1/3}Fe_{1/3}Co_{1/3}PO_4$

Atom	*x* (Å)	*y* (Å)	*z* (Å)	B_{iso}	Occupancy
Li1	0	0	0	0.2(4)	0.46
Fe	0.2734(6)	0.25	0.9800(14)	1.88(15)	0.356
Mn	0.2734(6)	0.25	0.9800(14)	1.88(15)	0.348
Co	0.2734(6)	0.25	0.9800(14)	1.88(15)	0.296
P	0.0947(3)	0.25	0.4124(6)	-	1
O1	0.1101(3)	0.25	0.7297(5)	-	1
O2	0.4506(3)	0.25	0.1783(5)	-	1
O3	0.1679(3)	0.0489(3)	0.2742(5)	-	1

Atom	U_{11} (Å^2)	U_{22} (Å^2)	U_{33} (Å^2)	U_{12} (Å^2)	U_{13} (Å^2)	U_{23} (Å^2)
P	0.0039(4)	0.0056(9)	0.006(2)	0	-0.0020(8)	0
O1	0.0046(4)	0.0068(9)	0.009(2)	0	0.0003(7)	0
O2	0.0025(4)	0.008(1)	0.016(2)	0	0.0026(5)	0
O3	0.0054(3)	0.0058(5)	0.007(1)	0.0029(3)	0.0012(5)	-0.0006(9)

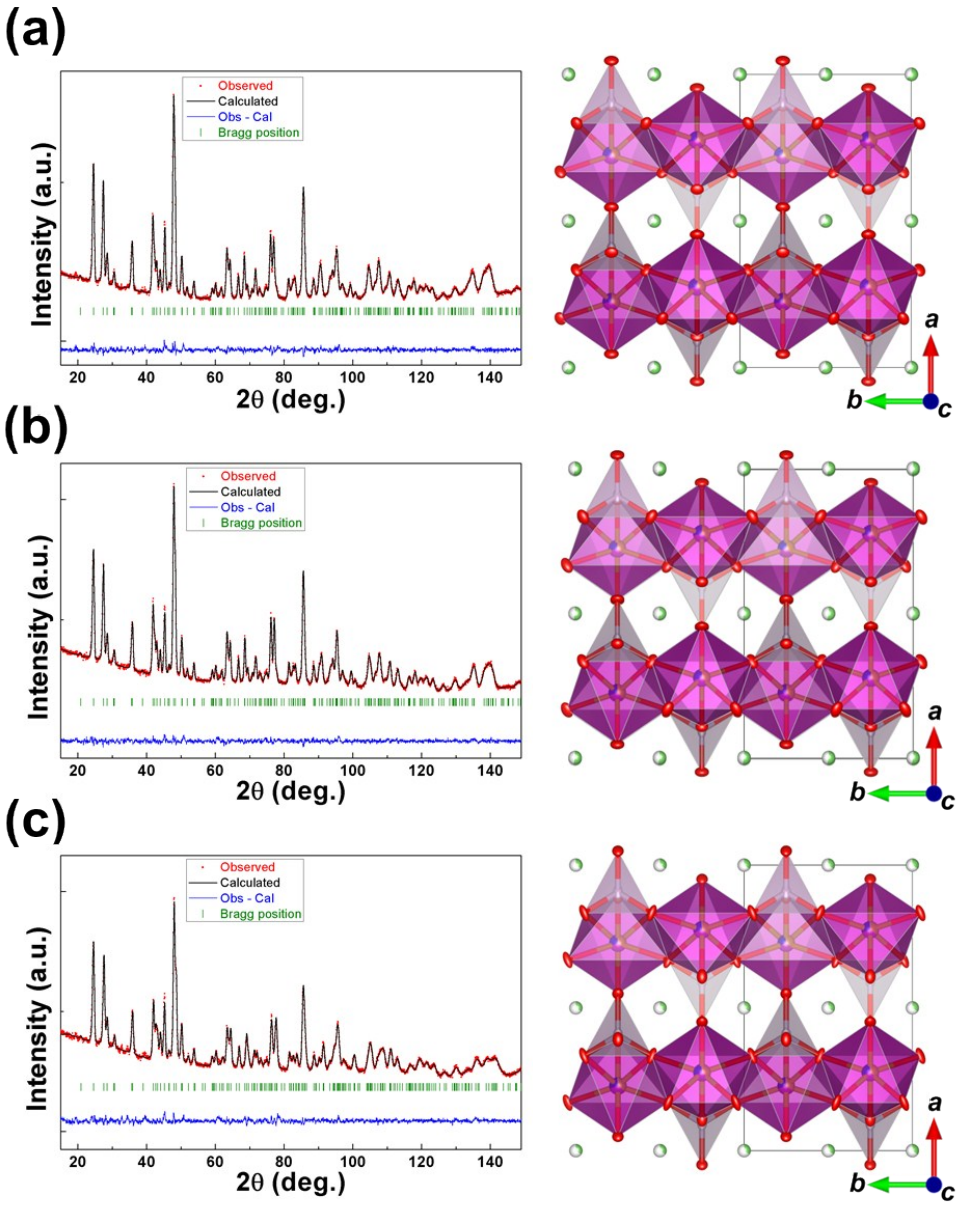

Fig. S5. Rietveld refinement of the neutron diffraction pattern of $Li_xMn_{1/3}Fe_{1/3}Co_{1/3}PO_4$ ((a) x = 2/3, (b) x = 1/2, (c) x = 1/3) at room temperature. The observed data, calculated profiles, difference between observed and calculated profiles and Bragg position are presented as red markers, black line, blue line and green markers, respectively. Schematic representations of each phase with the anisotropic thermal motion of each atom with 60 % probability are described beside neutron diffraction patterns. Thermal atomic Rietveld refinement of $Li_xFe_{1/3}Mn_{1/3}Co_{1/3}PO_4$ (x = 2/3, 1/2, 1/3) was satisfactory with low R-factors, and lattice

parameter and cell volume are in a good agreement with previous XRD results

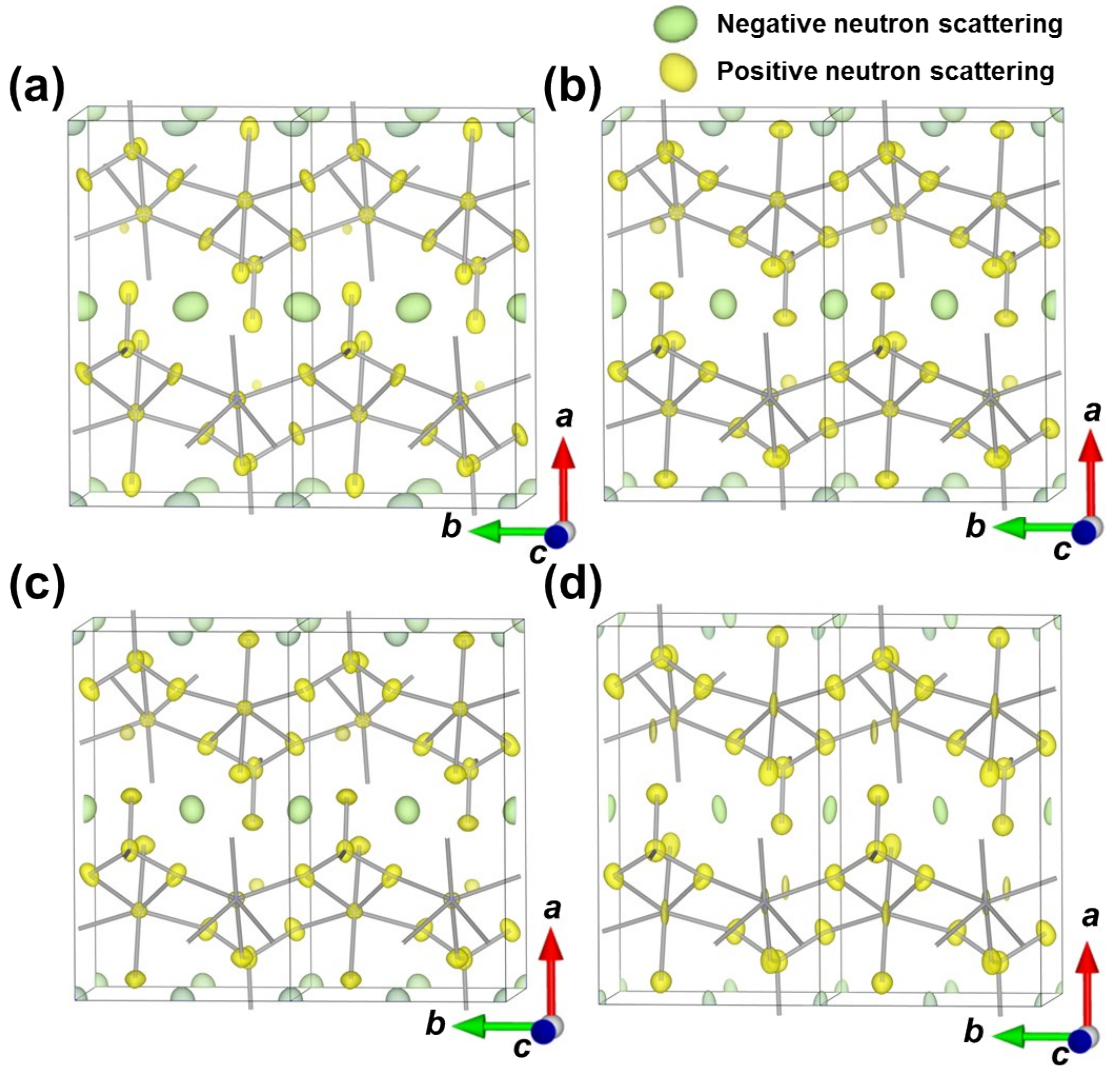

Fig. S6. Nuclear density maps of $Li_xMn_{1/3}Fe_{1/3}Co_{1/3}PO_4$ ((a) $x = 1$, (b) $x = 2/3$, (c) $x = 1/2$, (d) $x = 1/3$) using MEM. The nuclear density contours from the positive and negative scattering at the cut off range of -2.0 to 32 are shown as yellow and green colors, respectively.

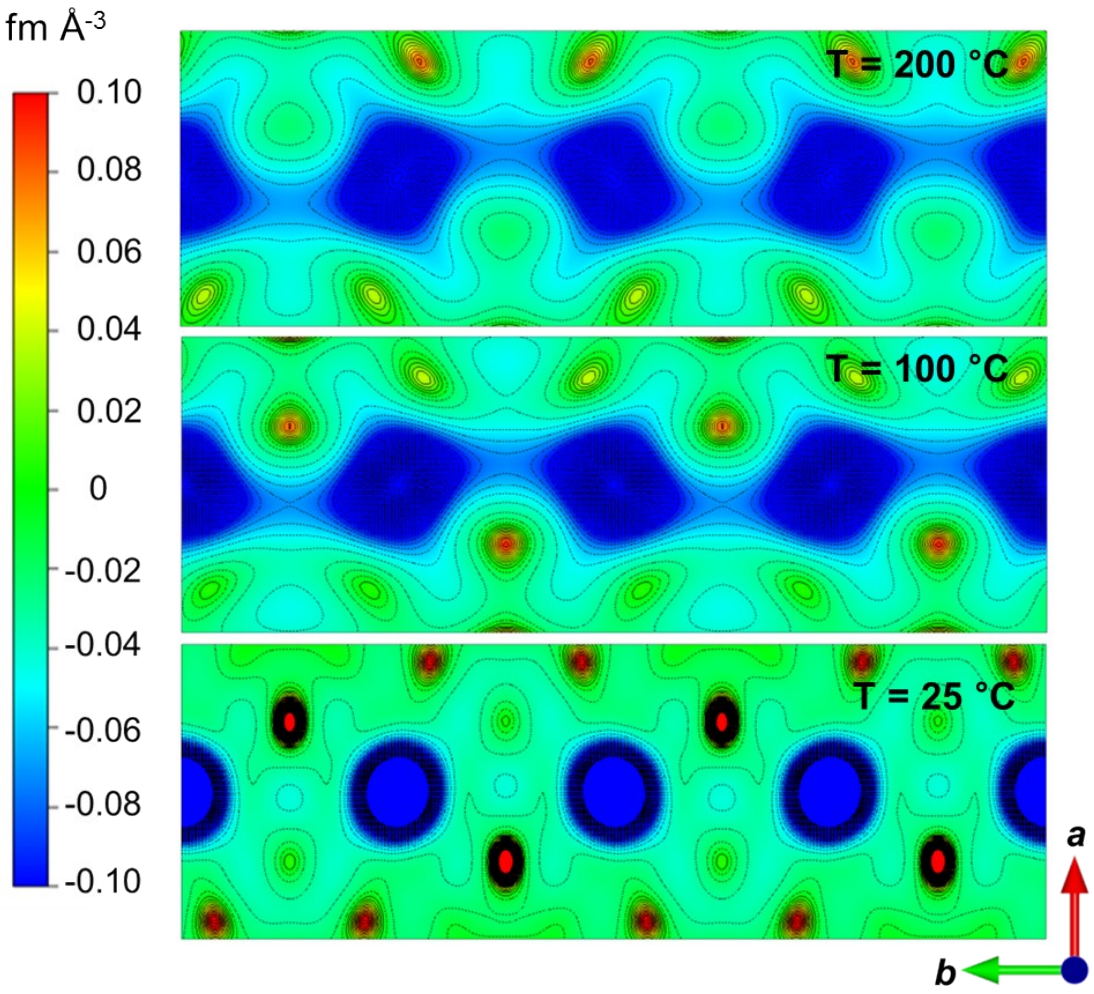

Figure S7. Two-dimensional nuclear density maps of $Li_{0.67}Mn_{1/3}Fe_{1/3}Co_{1/3}PO_4$ at various temperatures (T = 100, 200 and 300 °C) sliced on the (001) plane at z = 0.47.